Synthesis of Transparent Poly(vinylidene fluoride) (PVdF) / Zirconium Oxide Hybrids without Crystallization of PVdF Chains

Takeshi OTSUKA and Yoshiki CHUJO*

TOC Graphic

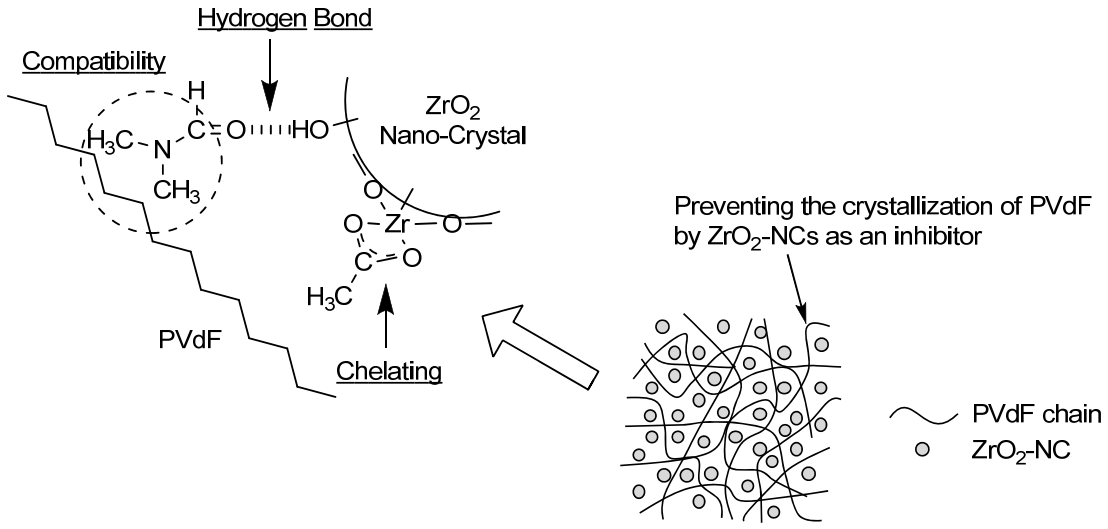

Synthesis of Transparent Poly(vinylidene fluoride) (PVdF) / Zirconium Oxide Hybrids without Crystallization of PVdF Chains

Takeshi OTSUKA[1,2] and Yoshiki CHUJO[2*]

[1] Sumitomo Osaka Cement Co., LTD. 585, Toyotomi-cho, Funabashi-shi, Chiba 274-8601, JAPAN

[2] Department of Polymer Chemistry, Graduate School of Engineering, Kyoto University, Katsura, Nishikyo-ku, 615-8510, JAPAN

[*] Corresponding author. Tel.: +81 75 383 2604; fax: +81 75 383 2605.

E-mail address: chujo@chujo.synchem.kyoto-u.ac.jp

Abstract

Transparent and homogeneous organic-inorganic hybrids with poly(vinylidene fluoride) (PVdF) could be prepared by addition of zirconium oxide nanocrystals (ZrO_2-NCs) in a polar aprotic solvent and the subsequent solvent evaporation. The polar aprotic solvents such as DMF, DMAc and DMSO would form hydrogen bonds with Zr-OH groups of the ZrO_2-NC and play a role as compatibilizers between the PVdF and ZrO_2-NCs. The interpenetration between PVdF and ZrO_2-NCs resulted in the nanometer dispersion of PVdF chains in a ZrO_2-NC matrix. High dosage of the ZrO_2-NCs as physical inhibitors between PVdF polymer chains sufficiently prevented the PVdF chain mobility in the internal of hybrids. The transparency of the PVdF/ZrO_2-NC hybrids was dramatically improved by controlling the content of ZrO_2-NCs. Novel multifunctional hybrids with high transparency, high refractive index and good mechanical property were obtained by hybridization of PVdF and ZrO_2-NCs.

Key Word: Poly(vinylidene fluoride), Zirconium Oxide, Nanocrystal, Polar Aprotic Solvent, Compatibilizer, Transparency, Organic-Inorganic Hybrid.

1. Introduction

Hybrid materials or nanocomposites have attracted a great deal of attention because of their high performance and unique property which cannot be achieved by other simple materials [1-5]. The hybrid materials from organic polymers and metal oxide offer different chemical and physical properties such as flame resistance, high transparency and excellent solvent resistance properties which were different from those of bulk materials [6-10]. In particular, transparency is one of the most striking features of the hybrid materials. Scattering loss is avoided due to the dispersion of components on the order of nanometers.

The most simple and convenient idea for the construction of transparent and homogeneous hybrid materials is an increasing affinity between organic polymer and inorganic phases. The organic-inorganic hybrid materials are generally prepared by utilizing two major types of interactions, namely covalent bond interactions and physical interactions. The introduction of covalent bond between organic polymer and silica gel accomplished the preparation of transparent hybrids with polystyrene [11], polyacrylates [12, 13], poly(dimethylsiloxane) (PDMS) [14, 15] and polysilane [16, 17]. Transparent hybrids using physical interactions such as hydrogen bonding [18, 19], aromatic [20] and ionic [21] interactions between organic polymer and silica gel have been also reported. On the other hand, a new concept of ‘‘compatibilizer’’ between organic polymers and silica gel was applied to obtain transparent hybrids by utilizing polar aprotic solvents [22] or cyclodextrin [23] as a compatibilizer.

The method of preparing transparent hybrid was developed by incorporating inorganic nanocrystals into polymer matrices [24]. Metal oxide nanocrystals are especially difficult to disperse homogeneously in organic polymers. To improve the miscibility of inorganic nanocrystals and organic polymers, the synthesis of metal oxide nanocrystals by non-aqueous sol-gel routes has been developed [25-29]. Organic groups attached to the surface of the nanocrystals might prevent the formation of aggregates and make their polarity adjustable to the medium.

Here, this article describes the synthesis of poly(vinylidene fluoride) (PVdF)/zirconium oxide nanocrystals (ZrO_2-NCs) hybrids using a polar aprotic solvent as a compatibilizer. PVdF is a very attractive polymer, exhibiting piezoelectric and

pyroelectric characteristics, which is applied for electronic devices [30-32]. However, the thermal and mechanical properties of PVdF are not so high due to its low glass transition temperature (T_g = -35 ºC). The reinforcement of PVdF with inorganic filler, which had excellent mechanical and thermal properties and hardness, has been extensively investigated. However, it is very hard and difficult to obtain transparent PVdF/metal oxide hybrid materials because of the high crystallinity of PVdF, the low solubility of PVdF in common organic solvents and the low surface energy of fluorine atom containing PVdF [33-35]. On the other hand, ZrO_2 nanocrystals have chemical inertness, excellent mechanical properties, high refractive index and thermal stability. Small particles less than 10nm can avoid Rayleigh scattering and be incorporated into a transparent polymer matrix. Only very few examples regarding the homogeneous dispersions of ZrO_2 nanocrystals have been reported. Recently, by utilizing an artifice of manufacture process, we got non-aggregated tetragonal ZrO_2 nanocrystals (3nm) in water solution [36, 37]. This ZrO_2 nanocrystal aqueous sol is colorless and suitable for preparation of polymer and zirconium oxide hybrid materials.

In this paper, the inhibition of crystallization of PVdF by ZrO_2 nanocrystals using polar aprotic solvents enabled the strong interaction between PVdF and ZrO_2 nanocrystals and the preparation of the transparent PVdF/ZrO_2 nanocrystal hybrids. In the view points of the new properties by hybridization with ZrO_2 nanocrystals at nanometer level, PVdF/ZrO_2 nanocrystal hybrids showed excellent transparency, high refractive index and superior mechanical property. The original crystallinity of PVdF decreased because of the hybridization with ZrO_2 nanocrystals at nanometer scale. The PVdF/silica hybrids utilizing sol-gel reaction have been reported by us [38]. However, it is the first example that transparent and homogeneous PVdF/ZrO_2 hybrids by using inorganic nanocrystals could be obtained. Therefore, they will be promisingly applied for optical functional materials and coatings.

2. Experimental Section

2.1. *Materials*

Poly(vinylidene fluoride) (M_n=71,000, M_w/M_n=2.53) was purchased from Aldrich. Zirconium oxide nanocrystal (ZrO_2-NC) aqueous sols, which contained 10.0wt% ZrO_2

with chloride anion (pH=2.0) and acetate anion (pH=1.7 and 2.5), were obtained from Sumitomo Osaka Cement Co., Ltd. N,N-Dimethylformamide (DMF) and N,N-dimethylacetamide (DMAc) were dried and distilled over magnesium sulfate under reduced pressure and stored under nitrogen. Dimethyl sulfoxide (DMSO) and the other reagents were used as supplied.

2.2. *Measurements*

Powder X-ray diffraction patterns (XRD) were recorded on a Mini Flex/AW (Rigaku) using Cu-K_α radiation (λ = 1.5406 Å). Fourier transform infrared (FT-IR) spectra were obtained using a Perkin Elmer 2000 infrared spectrometer by a KBr pellet method. Scanning electron microscopy (SEM) measurements were conducted using a JSM-5600B system (JEOL). The surface images were measured using a tapping mode atomic force microscopy (TM-AFM) (SPA 400, SEIKO Instruments Inc.) operating at room temperature. Height and phase images were recorded simultaneously. Nanoprobe cantilevers (SI-DF20, SEIKO Instruments Inc.) were utilized. Transmission electron microscopy (TEM) was performed with a JEM-2100F microscopy (JEOL) at 200 kV. Specimens were prepared cutting by use of focused ion beam (FIB) (SMI2050, SEIKO Instruments Inc.). Differential scanning calorimetry (DSC) thermograms were obtained with a DSC200 (SEIKO Instruments Inc.) at a heating rate of 10 ºC/min under nitrogen atmosphere. Thermogravimetric analysis (TGA) was performed using a TGA/DTA6200 (SEIKO Instruments Inc.) at a heating rate of 10 °C/min in air. The ^{1}H-NMR spectra were recorded on a 400 MHz EX-400 spectrometer (JEOL). Dimethyl sulfoxide-d_6 with 0.05vol% TMS was used in the liquid NMR measurements. UV-visible absorption spectra were measured with a model MPS-2000 multipurpose spectrometer (Shimadzu). The refractive index was determined by an Abbe refract-meter using a DR-M4 (ATAGO Co., Ltd.). Contact angle against water on a horizontal surface of a pellet was measured at 25 ºC with a Kyowa Kaimen Kagaku CAD type gonimeter. For the mechanical properties of hybrids, the pencil hardness was evaluated on spin coated samples according to the standard test methods ASTM D 3363.

2.3. *Synthesis of PVdF/ZrO_2-NC hybrids*

A typical preparation process of PVdF/ZrO_2-NC hybrids is as follows. The ZrO_2-NC

aqueous sol was dried by using evaporator to get a ZrO_2-NC powder. The obtained ZrO_2 powder was added into the solvent and stirred for 3 h at room temperature. PVdF was added to this solution and dissolved by heating. The resulting solution was allowed to cool at room temperature. Then, the resulting solution was placed in a polypropylene container and left in an oven at 60 ºC to evaporate the solvent. The resulting sample was dried in a vacuum oven at 80 ºC to remove the solvent.

2.4. *Post-treatment of hybrids to remove remained DMF*

After drying in a vacuum oven at 80 ºC, DMF still remained in the hybrids. The remained DMF in the hybrids could be completely dried using two post-treatments. One is solvent extraction with methanol using Soxhlet's extractor for 3 days, since DMF is widely miscible with methanol. The other is heating of hybrids at 80 ºC for 24 h.

3. Results and Discussion

3.1. *Synthesis of PVdF/ZrO_2-NC hybrids*

PVdF/ZrO_2-NC hybrids were prepared utilizing polar aprotic solvents such as DMF, DMAc and DMSO. The ZrO_2-NCs in the present study have tetragonal phase from XRD result. Application of Scherrer equation, [39] $t = 0.9\lambda/\beta\cos\theta_\beta$, where t is the crystallite size, λ is the wavelength of the radiation used, β is the pure diffraction breath and θ_β is the Bragg diffraction angle, enabled us to estimate that the crystallite size of ZrO_2-NC was 3 nm. ZrO_2-NCs aqueous sol, which has high transparency without the particle aggregation was characterized by our previous work [40]. At first, ZrO_2-NC powders modified with chloride anion (initial sol pH=2.0) or with small amount of acetate anion (initial sol pH=2.5) were used as an inorganic component for preparation of PVdF/ZrO_2-NC hybrids. But, in the samples using the ZrO_2-NC powders modified with 3.17wt% of chloride anion (Table 1, Run 2) or with 16.9 wt% of acetate anion (Table 1, Run 3), the ZrO_2-NCs were not dispersed into DMF and the precipitation of ZrO_2-NC gels appeared during the preparation of the hybrids. Especially, the ZrO_2-NC powders modified with chloride anion were not re-dispersed into any other solvents, such as water, alcohols or polar aprotic solvents, when once the solvents were removed from the initial sol. The hydrogen chloride-modified ZrO_2-NC powders which did not

have effective steric hindrance on the ZrO_2-NC surface attracted the aggregation of the ZrO_2-NCs. On the other hand, the ZrO_2-NC powders modified with acetate anion which depressed the nanocrystal aggregation by steric hindrance from acetate anion were re-dispersed easily into solvents. These results indicate that steric hindrance from the surface modifier, and hydrophilic and hydrophobic properties of the ZrO_2-NC surface are very important to obtain the homogeneous PVdF/ZrO_2-NC hybrids. Therefore, the more hydrophobic ZrO_2-NCs with 19.7 wt% of acetate anion (initial sol pH=1.7) were employed to control the gelation of the ZrO_2-NCs in polar aprotic solvents. The effect of the amount of ZrO_2-NC powders on the homogeneity of PVdF/ZrO_2-NC hybrids is reported in Table 1. Figure 1 illustrates the typical appearances of the PVdF/ZrO_2-NC hybrids. The sample with PVdF/ZrO_2-NC=50/50 (wt/wt) brought about turbid (Run 4, Scheme 1a). In the material with PVdF/ZrO_2-NC=30/70 (wt/wt) (Run 5), the homogeneity was slightly increased compared with the sample of Run 4 and the appearance of the sample was translucent. With further addition of the ZrO_2-NCs, the appearance of hybrids was completely transparent (Run 6, Scheme 1b). These observations indicate that the transparency of the obtained hybrids was markedly improved with increasing of the amount of the ZrO_2-NCs used. As a control experiment, the sample without the ZrO_2-NCs (Run 1) became turbid. It is because the ZrO_2-NCs as an inhibitor were not incorporated between PVdF chains, high crystallinity of PVdF and the low surface energy of fluorine atom containing PVdF resulted in aggregation of PVdF. From these results, it was found that the physical inhibitors between PVdF polymer chains sufficiently prevented the aggregation of PVdF/ZrO_2-NC hybrids.

In different polar aprotic solvents, PVdF/ZrO_2-NC hybrids were also prepared. The employed solvents were DMF, DMAc and DMSO. The results are shown in Table 2. The appearances of PVdF/ZrO_2-NC hybrids were translucent when PVdF/ZrO_2-NC ratio was 70/30 (wt/wt) using DMF, DMAc or DMSO as the solvent (Table 2, Runs 5, 8, 10). In contrast, the PVdF/ZrO_2-NC hybrids with high amount of the ZrO_2-NCs using DMF, DMAc or DMSO as the solvent (Table 2, Runs 6, 9, 11) were transparent. In this way, the composition of PVdF and ZrO_2-NCs was crucial to obtain transparent hybrids, which were favorable high amount of the ZrO_2-NCs. The ceramic contents of PVdF/ZrO_2-NC hybrids determined by TGA were good agreement with the calculated values (Table 2, Runs 6, 9, 11).

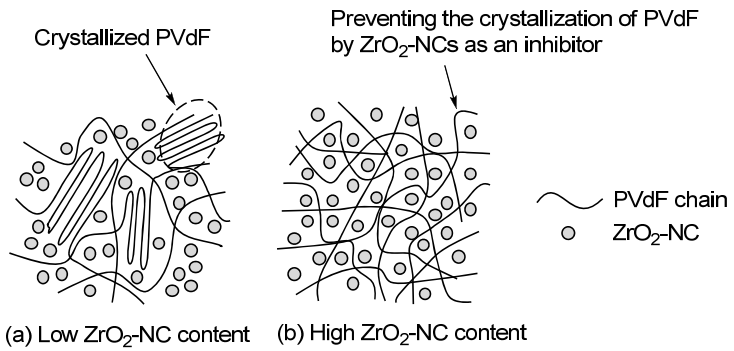

Scheme 1. Schematic representation of structural change for PVdF/ZrO_2-NC hybrids.

Table 1 Synthesis of PVdF/ZrO_2-NC hybrids

Run	PVdF/ZrO_2-NC ratio (wt/wt)	PVdF (g)	Surface modifier on ZrO_2-NC	ZrO_2-NCs with surface modifier (g)	Solvent	Appearance
1	100/0	0.70	-	0.00	DMF 3ml	Turbid
2	50/50	0.50	Cl^-	0.52 [a)]	DMF 3ml	Gelation
3	50/50	0.50	CH_3COO^-	0.60 [b)]	DMF 3ml	Gelation
4	50/50	0.50	CH_3COO^-	0.62 [c)]	DMF 3ml	Turbid
5	30/70	0.30	CH_3COO^-	0.87 [c)]	DMF 3ml	Translucent
6	20/80	0.20	CH_3COO^-	1.00 [c)]	DMF 3ml	Transparent
7	10/90	0.10	CH_3COO^-	1.12 [c)]	DMF 3ml	Transparent

a) The amount of chloride anion was 3.17 wt% measured by elemental analysis. Initial sol pH was 2.0.

b) The amount of acetate anion was 16.9 wt% by TGA. Initial sol pH was 2.5.

c) The amount of acetate anion was 19.7 wt% by TGA. Initial sol pH was 1.7.

Table 2 Synthesis of PVdF/ZrO_2-NC hybrids using various polar aprotic solvents

Run	PVdF/ZrO_2-NC ratio (wt/wt)	PVdF (g)	ZrO_2-NCs with surface modifier [a)] (g)	Solvent	Appearance	Ceramic yield (%)	
						Calcd.	Obsd. [c)]
5	30/70	0.30	0.87	DMF 3ml	Translucent	-	-
6	20/80	0.20	1.00	DMF 3ml	Transparent	66.9	66.1
8	30/70	0.30	0.87	DMAc 3ml	Translucent	-	-
9	20/80	0.20	1.00	DMAc 3ml	Transparent	66.9	65.5
10	30/70	0.30	0.87	DMSO [b)] 3ml	Translucent	-	-
11	20/80	0.20	1.00	DMSO [b)] 3ml	Transparent	66.9	65.0

a) The amount of acetate anion was 19.7 wt% by TGA. Initial sol pH was 1.7.

b) Evaporated solvent at 100 ºC in air and dried at 120 ºC in vacuum.

c) Determined by TGA. The samples after two post-treatments were used.

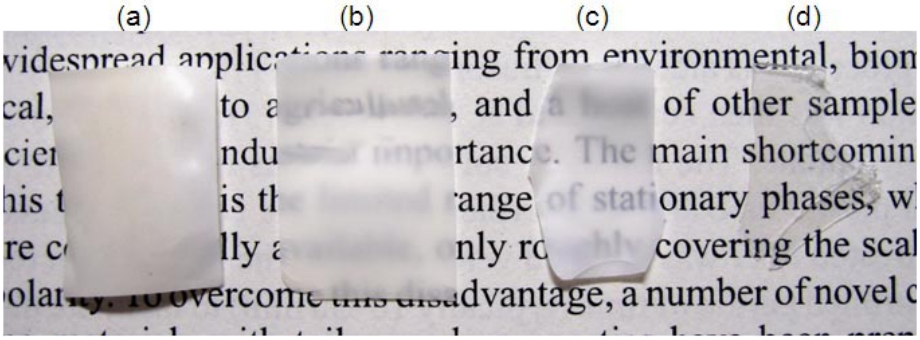

Figure 1. Photograph of (a) the pristine PVdF (Run 1), (b) Run 4 (PVdF/ZrO_2-NC=50/50), (c) Run 5 (PVdF/ZrO_2-NC=30/70) and (d) Run 6 (PVdF/ZrO_2-NC=20/80).

3.2. *Morphology of PVdF/ZrO_2-NC hybrids*

The homogeneity of the obtained PVdF/ZrO_2-NC hybrid was investigated by SEM. In Run 1, the surface of the pristine PVdF was uncontinuous structure (Figure 2a) resulted from aggregation of PVdF. The turbid sample (Run 4) was found to show aggregation on a micro scale. In contrast, the translucent sample (Run 5) showed the white precipitates at 5,000 magnifications (Figure 2c). The white precipitates indicate ZrO_2-NCs' aggregate. As shown in Figure 1d, the white precipitates clearly disappeared in the transparent hybrids (Run 6). These results strongly indicate that the miscibility of PVdF/ZrO_2-NC hybrids containing high dosage of ZrO_2-NCs is a nanometer level.

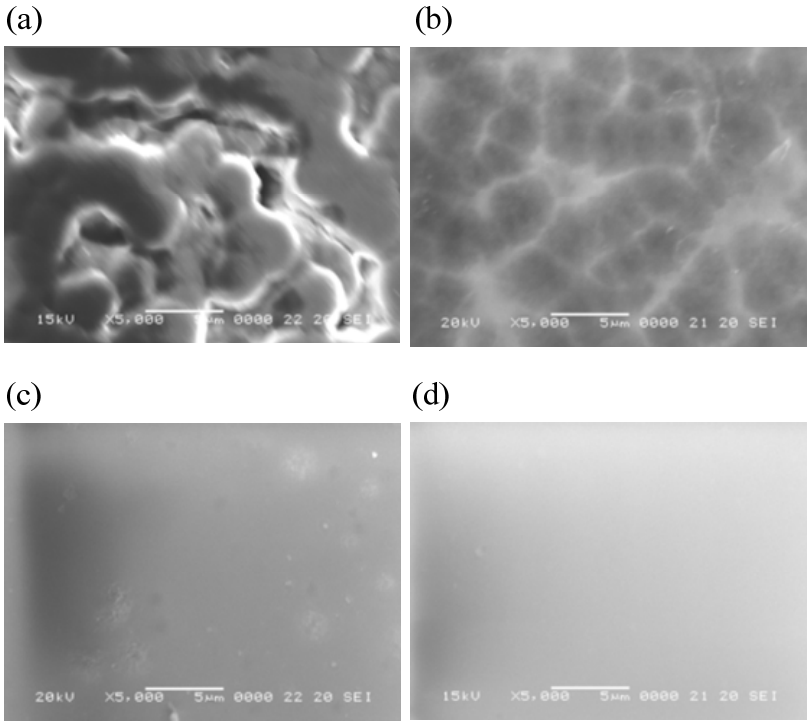

Figure 2. SEM images of (a) the pristine PVdF (Run 1), (b) Run 4 (PVdF/ZrO_2-NC=50/50), (c) Run 5 (PVdF/ZrO_2-NC=30/70) and (d) Run 6 (PVdF/ZrO_2-NC=20/80).

3.3. *Crystallinity of PVdF in PVdF/ZrO_2-NC hybrids*

The crystallinity of PVdF in ZrO_2-NC matrix was investigated by XRD. The pristine PVdF exhibited high crystallinity as shown in Figure 3a. But, the crystallinity of PVdF was gradually decreasing with increasing of ZrO_2-NC contained and the sharp peaks could be assigned to a tetragonal ZrO_2 structure (Run 4). In the transparent hybrid (Run 6), the characteristic peaks of PVdF clearly disappeared and the sharp peaks attributable to tetragonal ZrO_2 were confirmed. These results indicate the molecular scale dispersion of PVdF in the ZrO_2-NC matrix.

The crystallinity of PVdF in PVdF/ZrO_2-NC hybrids was also checked by DSC measurement (Figure 4). The endothermic peak between 110 and 180 ºC corresponds to the melting of the crystalline PVdF. From DSC thermograms it was observed that the amount of ZrO_2-NCs influences the crystalline melting temperature (T_m), heat of fusion (ΔH_m) and crystallinity (X_c). Thermodynamic properties of PVdF/ZrO_2-NC hybrids obtained from DSC measurement are summarized in Table 3. The percentage of

crystalline PVdF (X_c) can be calculated with the equation $X_c=\Delta H_m/\Delta H^*_m$, where ΔH^*_m is the melting enthalpy of a completely crystalline PVdF. It can be seen from Table 3 that both the melting temperature (T_m) and X_c decrease with an increase of ZrO_2-NC content in agreement with the XRD results.

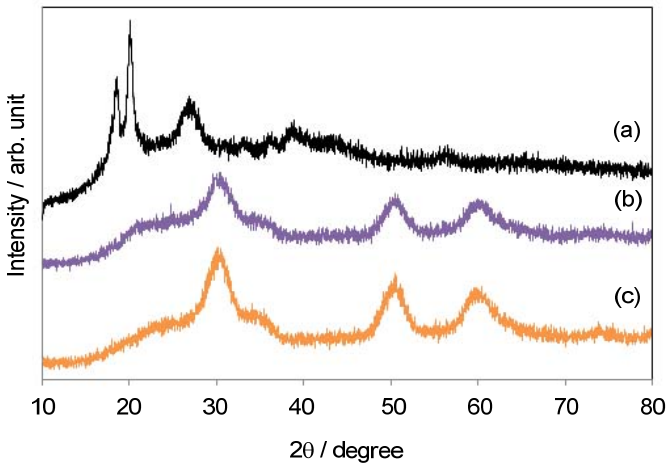

Figure 3. XRD patterns of (a) the pristine PVdF (Run 1), (b) Run 4 (PVdF/ZrO_2-NC=50/50) and (c) Run 6 (PVdF/ZrO_2-NC=20/80).

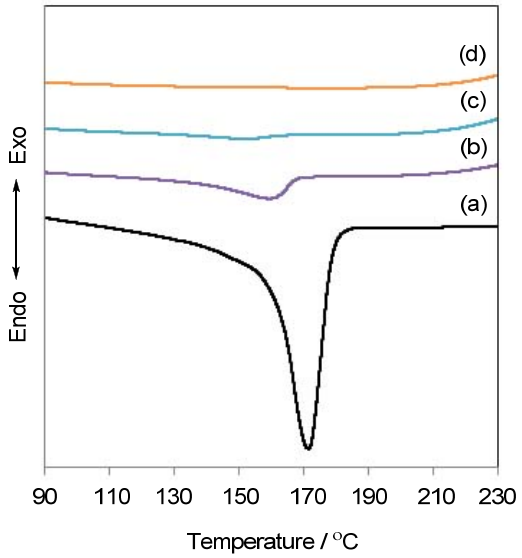

Figure 4. DSC thermograms of (a) the pristine PVdF (Run 1), (b) Run 4 (PVdF/ZrO_2-NC=50/50), (c) Run 5 (PVdF/ZrO_2-NC=30/70) and (d) Run 6 (PVdF/ZrO_2-NC=20/80).

Table 3. Thermodynamic properties of PVdF/ZrO_2-NC hybrids

Run	PVdF/ZrO_2-NC ratio (wt/wt)	T_m (ºC)	ΔH_m (J/g)	X_c [a)] (%)
1	100/0	160.0	58.6	55.8
4	50/50	133.5	12.9	12.3
5	30/70	125.7	2.08	1.98
6	20/80	-	～0	～0

a) $X_c = (\Delta H_m/\Delta H^*_m)\times 100$, $\Delta H^*_m = 105$ (J/g) [41].

3.4. *Chemical structures of PVdF/ZrO_2-NC hybrids*

The hydrogen bonding interaction between a polar aprotic solvent and the surface Zr-OH of the ZrO_2-NCs was confirmed by FT-IR measurement. It was recognized that the stretching band of the amide carbonyl peaks of the polar aprotic solvent in the hybrids was shifted to lower wavenumbers compared to that of bulk polar aprotic solvent due to the strong hydrogen bonding interaction. As shown in Figure 5, in the case of the sample after vacuum drying of the transparent PVdF/ZrO_2-NC hybrids using DMF (Table 1, Run 6) at 80 ºC for 24h, the amide carbonyl stretching band of DMF was observed (Figure 5a). DMF was incorporated and remained in the hybrids because of the hydrogen bonds with the Zr-OH groups, while DMF was easily evaporated under vacuum drying conditions. This result means that DMF formed the strong hydrogen bonds with Zr-OH groups of the ZrO_2-NCs. The amide carbonyl band of DMF in the hybrids was shifted from 1668 cm^{-1} (bulk DMF, Figure 5a) to 1651 cm^{-1}. The schematic representation of mechanism to prepare the PVdF/ZrO_2-NC hybrid is shown in Scheme 2. ZrO_2 may have active sites, i.e. the Brönsted acid site (Zr-OH) is modified by acetic acid. On the other hand, DMF has amide carbonyl groups. A hydrogen bond between Zr-OH groups of ZrO_2-NCs and the amide carbonyl groups of DMF plays an important role in stabilizing and dispersing ZrO_2-NCs in solutions and in bulk hybrid materials.

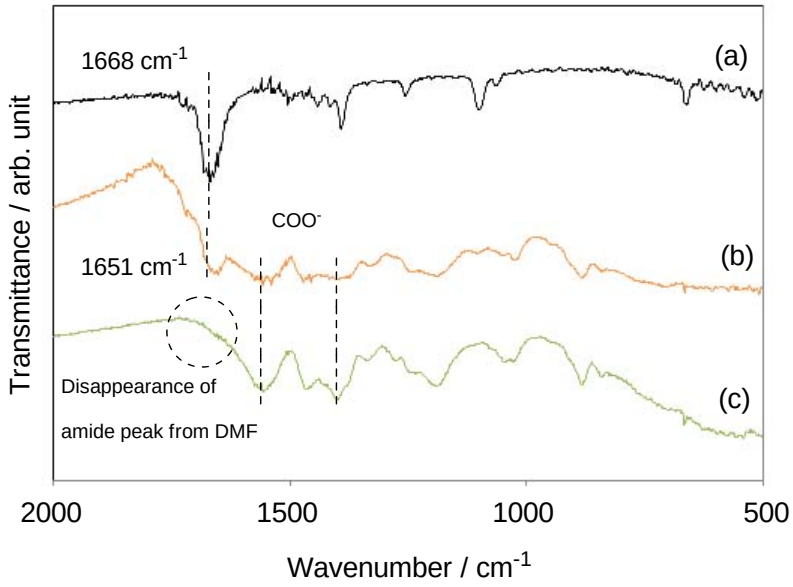

Figure 5. FT-IR spectra of (a) DMF, (b) Run 6 (PVdF/ZrO_2-NC=20/80) and (c) Run 6 (PVdF/ZrO_2-NC=20/80) after post-treatment (using solvent extraction with methanol).

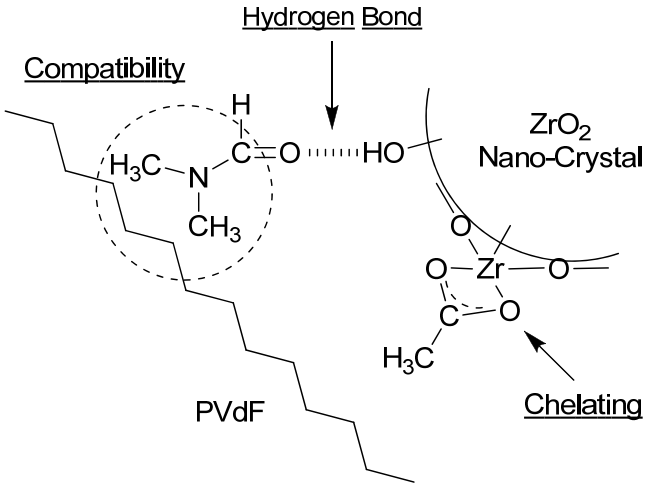

Scheme 2. Schematic representation of mechanism to prepare PVdF/ZrO_2-NC hybrid.

3.5. *Post treatment of PVdF/ZrO_2-NC hybrids*

Furthermore, two post-treatments were performed to remove the remained DMF in the hybrids completely: (i) DMF extraction with methanol for 3 days and (ii) heating of hybrids at 80 ºC for 24 h. Using both methods, the remained DMF in the hybrids was completely removed. As shown in Figure 5c, the amide carbonyl band of DMF in hybrids disappeared in both cases. Figure 6 shows the ^{1}H-NMR spectra of transparent

PVdF/ZrO_2-NC hybrids (Table 1, Run 6) before and after post treatment. After solvent extraction with methanol and heating of hybrids, the peaks of DMF proton (the peaks of a, a' and b, δ= 2.73, 2.89, 7.95 ppm) completely disappeared. The result indicates the complete removing of the remained DMF in PVdF/ZrO_2-NC hybrids. The characteristic broad peak around 8.5 ppm was found (Figure 6a). This is a peak derived from Zr-OH protons, which is also observed in the ^{1}H-NMR measurement of ZrO_2 powder with acetate anion (initial pH = 1.7) in DMSO. It was confirmed that the ^{1}H-NMR result supported the schematic representation of mechanism to prepare the PVdF/ZrO_2-NC hybrid (Scheme 2).

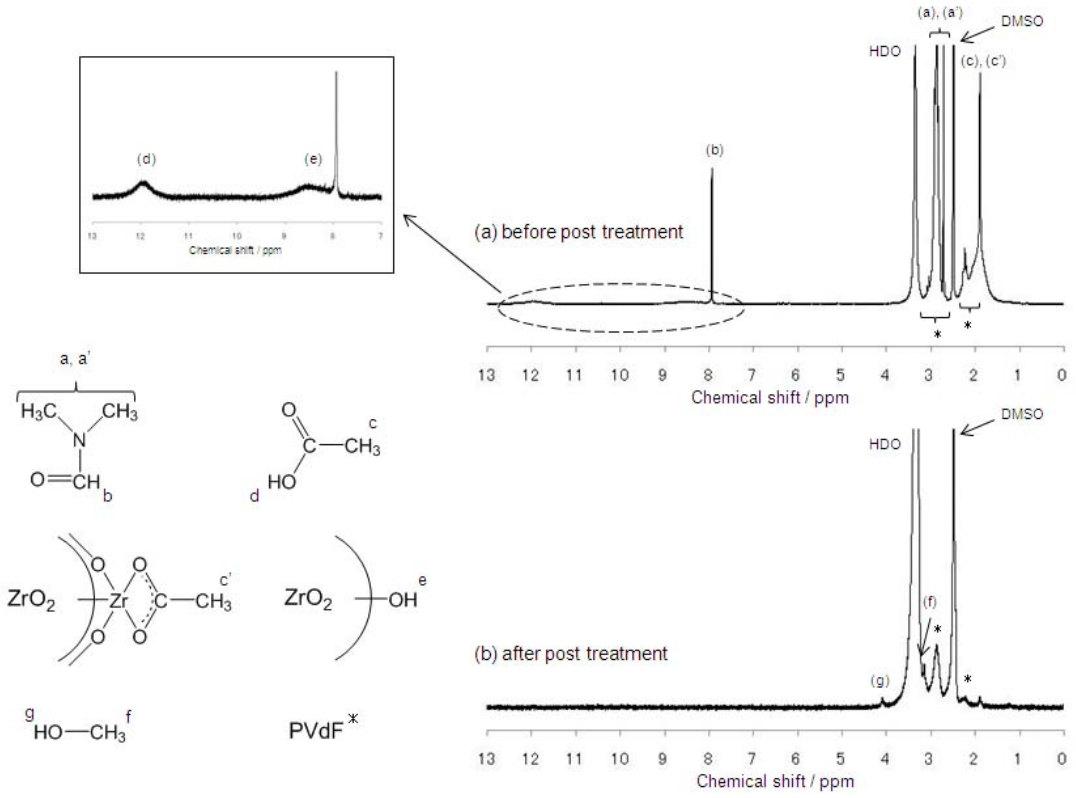

Figure 6. ^{1}H-NMR spectra of (a) Run 6 (PVdF/ZrO_2-NC=20/80) and (b) Run 6 (PVdF/ZrO_2-NC=20/80) after two post-treatments (using solvent extraction with methanol and heating) (in DMSO).

The surface morphology change of the hybrid before and after post treatment was investigated by TM-AFM. The surface roughness of the transparent hybrid before post treatment (Table 1, Run 6) was extremely smooth and flat (the roughness was less than

10 nm, Figure 7c). But, the transparency of the hybrids was changed by post-treatment. The surface roughness of the transparent hybrid after two post treatments (Table 1, Run 6, using solvent extraction with methanol and heating) was about 50 nm (3D height, Figure 7f). The appearance of the hybrid changed transparent to haze (almost transparent) using two post-treatments and crinkled surface morphology was observed by TM-AFM (Figure 7f).

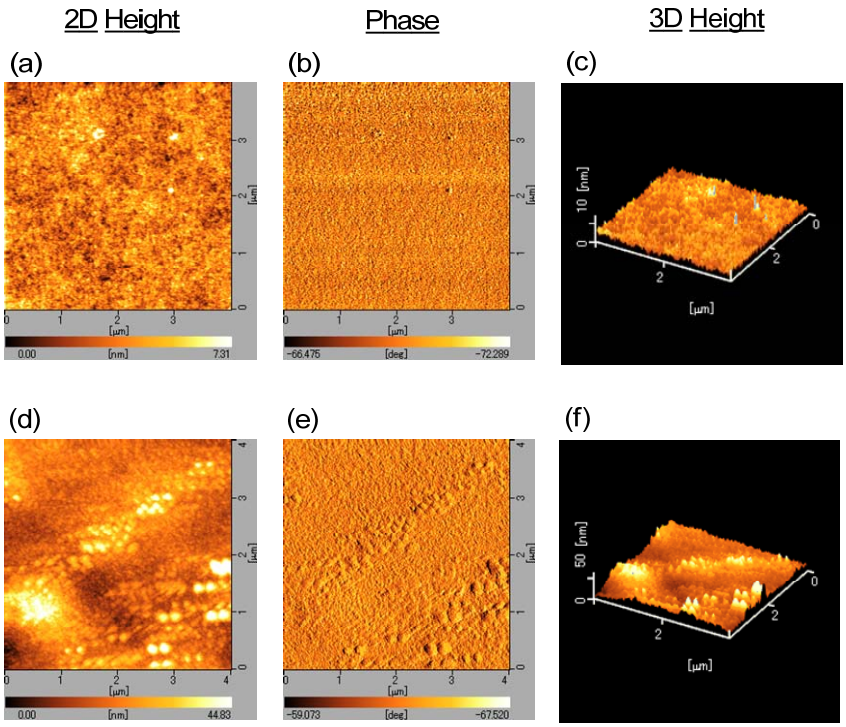

Figure 7. TM-AFM images of PVdF/ZrO_2-NC hybrids (a-c) Run 6 (PVdF/ZrO_2-NC=20/80) and (d-f) Run 6 (PVdF/ZrO_2-NC=20/80) after two post-treatments (using solvent extraction with methanol and heating). (a, d: 2D height; b, e: phase; and c, f: 3D height images).

To elucidate surface and internal morphologies of the obtained hybrid, the TEM was conducted on the transparent PVdF/ZrO_2-NC hybrids. Figure 8 shows images for cross section of the hybrids before and after post treatment. As shown in Figure 8a and 8b, the surface morphological change from flat to crinkling was also confirmed. On the other hand, Figure 8c and 8d confirms no difference between the hybrid before and after post treatment except for concave pattern (Figure 8c) which might be caused by evaporation of the remaining DMF in the hybrid. This result indicates that high dosage of the

ZrO_2-NCs as physical inhibitors between PVdF polymer chains sufficiently prevented the PVdF chain mobility in the internal of hybrid. Thus, the morphology change appeared to take place only on the bulk surface. It is because the physical entrapment of PVdF by the ZrO_2-NCs deterred the polymer aggregation. These TM-AFM and TEM observations also suggest the nano-scale miscibility between PVdF and ZrO_2-NCs.

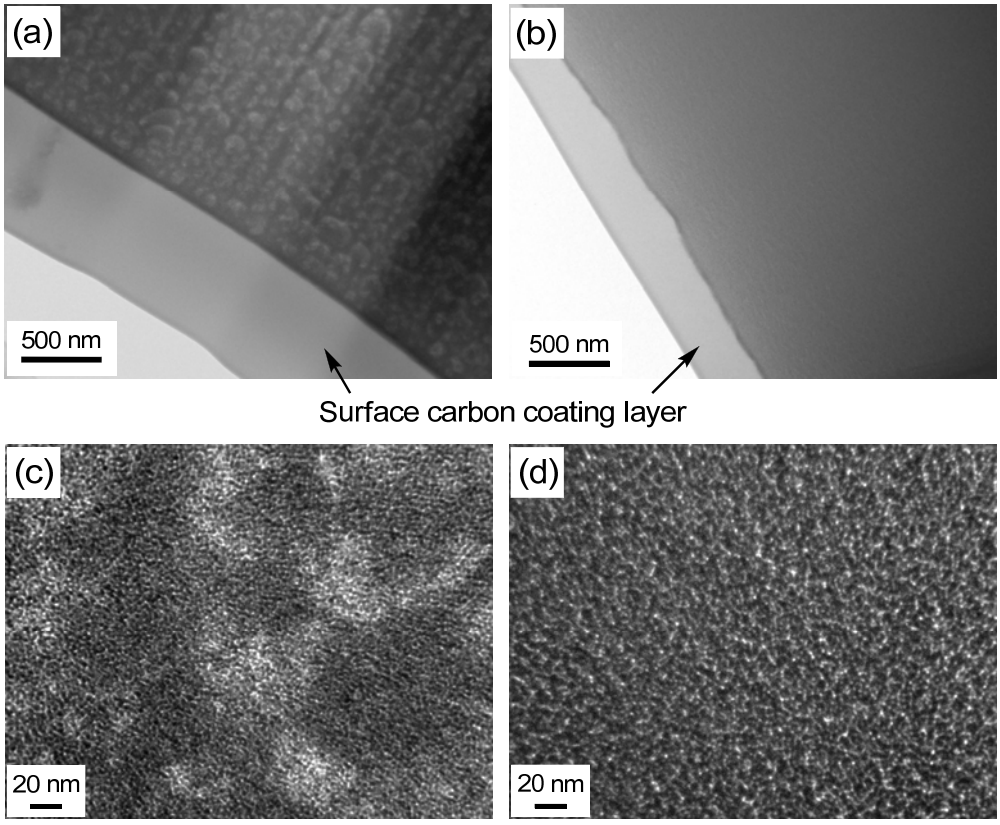

Figure 8. TEM images of PVdF/ZrO_2-NC hybrids (a, c) Run 6 (PVdF/ZrO_2-NC=20/80) and (b, d) Run 6 (PVdF/ZrO_2-NC=20/80) after two post-treatments (using solvent extraction with methanol and heating).

3.6. *Properties of PVdF/ZrO_2-NC hybrids*

Optical transparency of PVdF/ZrO_2-NC hybrid films was characterized by UV-vis spectra. Figure 9 shows the optical transmittance of a quartz glass substrate coated with about 5 μm thick of PVdF/ZrO_2-NC hybrid films (Table 1, Runs 1, 4 and 6). The films were formed on only one side of the substrate by spin coating. The turbid film (Run 4) was less transparent than the pristine PVdF because of light scattering from the

aggregation attributed to phase separation between PVdF and ZrO_2-NCs. On the other hand, it is observed that optical transmittance of the transparent PVdF/ZrO_2-NC hybrid film (Figure 9c) was higher than 85% in the visible light region, although it falls by crystallization of PVdF (Figure 9a and 9b). This result also confirms that the ZrO_2-NCs were uniformly distributed in the transparent hybrids and PVdF chains' aggregation was sufficiently prevented by the ZrO_2-NCs.

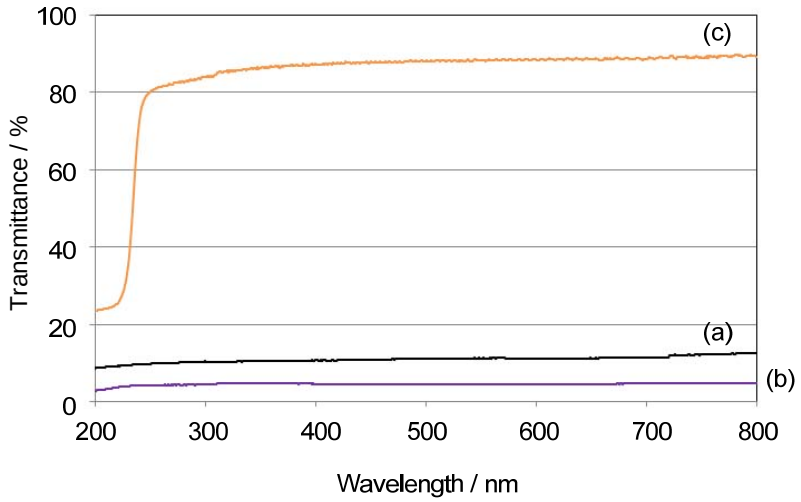

Figure 9. Optical transmittance of (a) the pristine PVdF (Run 1), (b) Run 4 (PVdF/ZrO_2-NC=50/50) and (c) Run 6 (PVdF/ZrO_2-NC=20/80).

The refractive index of the transparent hybrid film (Table 1, Run 6) as determined by Abbe refract-meter is shown in Table 4. The refractive index at 589 nm of the PVdF/ ZrO_2-NC hybrid film increased from 1.42 to 1.63 with the weight content of ZrO_2-NCs from 0 to 66wt% (Run 6). The obtained PVdF/ZrO_2-NC hybrid showed hydrophobicity. The contact angle of the PVdF/ZrO_2-NC hybrid (Run 6, after two post-treatments) was 72.2°, while the pure ZrO_2 bulk ceramic with polished surface was hydrophilic (56.9º). The incorporation of hydrophobic PVdF at a nanometer level gave the hydrophobic PVdF/ZrO_2-NC hybrid materials. Pencil hardness was taken into account as mechanical properties. The dependence of pencil hardness on hybrid coatings is shown in Table 4. Obviously, pencil hardness of PVdF/ZrO_2-NC hybrid coatings was higher than that of PVdF coating (not containing ZrO_2-NCs). In this paper, we utilized the single nano-sized ZrO_2 crystals so that hybrid materials with not only high transparency and

refractive index but also high hardness could be obtained by hybridization of PVdF and ZrO_2-NCs.

Table 4 Various properties of PVdF/ZrO_2-NC hybrids

Run	PVdF/ZrO_2-NC ratio (wt/wt)	Refractive index (@589 nm)	Contact angle [a)] (°)	Pencil hardness [d)]
1	100/0	1.42 [b)]	109.2	1H
6	20/80	1.63	72.2	6H
(ZrO_2)	0/100	2.20 [c)]	56.9	-

a) The sample after solvent extraction with methanol and annealing was used.

b), c) Obtained from literature [42, 43].

d) The film thickness on glass substrate was approximately 3μm.

4. Conclusion

Transparent and homogeneous hybrids were obtained in polar aprotic solvents such as DMF, DMAc and DMSO, which were used as a compatibilizer between the PVdF and ZrO_2-NCs. The polar aprotic solvents formed strong hydrogen bonds with the Zr-OH moieties and showed a high compatibility with the PVdF. The transparency of the PVdF/ZrO_2-NC hybrids was dramatically improved by controlling the content of ZrO_2-NCs. The interpenetration between PVdF and ZrO_2-NCs resulted in the nanometer dispersion of PVdF chains in a ZrO_2-NC matrix. The obtained PVdF/ZrO_2-NC hybrid was hydrophobic because of the incorporation of PVdF into ZrO_2-NC matrix at a nanometer level. Multifunctional hybrid materials with high transparency, high refractive index and good mechanical property were obtained by hybridization of PVdF and inorganic nanocrystals.

References

[1] Frissell WJ. In: Encyclopedia of Polymer Science and Technology. Bikales NM ed. vol. 6. New York: London: Sydney: John Wiley & Sons Inc, 1967. pp. 740.

[2] Special issues for organic-inorganic nanocomposite materials. Chem Mater 1996;

8(8), Chem Mater 1997; 9(11), Chem Mater 2001; 13(10).
[3] Schmid G, Maihack V, Lantermann F, Peschel S. J Chem Soc Dalton Trans 1996; 589.
[4] Beecroft LL, Ober CK. Chem Mater 1997; 9: 1302.
[5] Sanchez C, Lebeau B, Chaput F, Boilot JP. Adv Mater 2003; 15: 1969.
[6] Wen J, Wilkes GL. Chem Mater 1996; 8: 1667.
[7] Loym DA, Shea KJ. Chem Rev 1995; 95: 1431.
[8] Novak BM. Adv Mater 1993; 5: 422.
[9] Giannelis EP. Adv Mater 1996; 8: 29.
[10] Chujo Y, Tamaki R. MRS Bull 2001; 26: 389.
[11] Wei Y, Yang DC, Tang LG, Hutchins MK. J Mater Res 1993; 8: 1143.
[12] Wei Y, Wang W, Yeh JM, Wang B, Yang D, Murray JK Jr. Adv Mater 1994; 6: 372.
[13] Wei Y, Jin D, Brennan DJ, Rivera DN, Zhuang Q, DiNardo NJ, Qiu K. Chem Mater 1998; 10: 769.
[14] Sur GS, Mark JE. Eur Polym J 1985; 21: 1051.
[15] Huang HH, Orler B, Wikes GL. Macromolecules 1987; 20: 1322.
[16] Matsuura Y, Miura S, Naito H, Inoue H, Matsukawa K. J Organomet Chem 2003; 685: 230.
[17] Matsuura Y, Kumon K, Tohge N, Inoue H, Matsukawa K. Thin Solid Films 2002; 422: 4.
[18] Saegusa T, Chujo Y. Macromol Symp 1992; 64: 1.
[19] Chujo Y, Ihara E, Kure S, Saegusa T. Macromolecules 1993; 26: 5681.
[20] Tamaki R, Samura K, Chujo Y. Chem Commun 1998; 1131.
[21] Tamaki R, Chujo Y. J Mater Chem 1998; 8: 1113.
[22] Ogoshi T, Chujo Y. Bull Chem Soc Jpn 2003; 76: 1865.
[23] Ogoshi T, Chujo Y. Macromolecules 2003; 36: 654.
[24] Rong MZ, Zhang MQ, Zheng YX, Zeng HM, Walter R, Friedrich K. Polymer 2001; 42: 167.
[25] Niederberger M, Granweitner G. Chem Eur J 2006; 12: 7282.
[26] Niederberger M, Granweitner G, Krumeich F, Nesper R, Colfen H, Antoniettei M. Chem Mater 2004; 16: 1202.
[27] Pinna N, Grancharov S, Beato P, Bonville P, Antonietti M, Niederberger M. Chem

Mater 2005; 17: 3044.
[28] Ba JH, Polleux J, Antonietti M, Niederberger M. Adv Mater 2005; 17: 2509.
[29] Zhou S, Garnweitner G, Niederberger M, Antonietti M. Langmuir 2007; 23: 9178.
[30] Wang TT, Herbert JM, Glass AM. In: The Application of Ferroelectric Polymers. London: Blackie & Sons Ltd., 1988.
[31] Nalwa HS. Ferroelectric Polymers, Part I. New York: Marcel Dekker, 1995.
[32] Geschke D, Leister N, Steffen M, Glasel HJ, Hartmann EJ. Mater Sci Lett 1997; 16: 1943.
[33] Kim JW, Cho WJ, Ha CS. J Polym Sci Part B Polym Phys 2002; 40: 19.
[34] Tajitsu Y, Yonezawa M, Sato A, Tomiyama H, Date M, Fukada E, Yamashita Y. Jpn J Appl Phys 2000; 39: 5672.
[35] Cho JW, Sul KI. Polymer 2001; 42: 727.
[36] Kinoshita T. Japanese patent, JP P2006-016236A.
[37] Kinoshita T, Kawase T. Japanese patent, JP P2007-099931A.
[38] Ogoshi T, Chujo Y. J Polym Sci Part A Polym Chem 2005; 43: 3543.
[39] Cullity BD, Stock SR. Elements of X-ray Diffraction, 3rd ed. Pearson, Prentice Hall, Upper Saddle River, New Jersey, 2001.
[40] Otsuka T, Chujo Y. Poym J 2008; 40: 1157.
[41] Wunderlich B. Macromolecular Physics 3. Academic Press, 1980. pp. 50.
[42] Seferis JC ed. Polymer Handbook, 3rd ed. New York: John Wiley & Sons Inc., 1989.
[43] Samsonov GV ed. The Oxide Handbook, 2nd ed. New York: IFI/Plenum, 1982.